Comprehensive *Ab Initio* Quantum Mechanical and Molecular Orbital (MO) Analysis of Cisplatin: Structure, Bonding, Charge Density, and Vibrational Frequencies

P. N. V. PAVANKUMAR, P. SEETHARAMULU, S. YAO, JEFFREY D. SAXE, DASHARATHA G. REDDY, FREDERICK H. HAUSHEER

BioNumerik Pharmaceuticals, Inc., 8122 Datapoint Drive, Suite 1250, San Antonio, Texas 78229

Received 26 December 1997; accepted 20 October 1998

ABSTRACT: We carried out an extensive series of *ab initio* quantum mechanical (QM) calculations using pure effective core potential (ECP) and hybrid Hartree–Fock (HF)/ECP basis sets, including various electron correlation treatments up to the MP4 level on *cis*-diamminedichloroplatinum(II), cisplatin, an important anticancer drug. The optimized geometric parameters and vibrational frequencies of cisplatin were compared with the experimental values, and the effects of varying basis sets and correlation (MP level) treatments on the geometric parameters and vibrational frequencies were analyzed. We also present a detailed description of the bonding in cisplatin using qualitative MO analysis to characterize the key intramolecular interactions in cisplatin. The calculated molecular electrostatic potential (MEP), and the electrostatic potential (ESP) charges for cisplatin were used to identify regions of electrophilic and nucleophilic character. The charge density and the Laplacian of charge density of cisplatin were calculated to determine its bonding relationships. Using basis set performance, we identified two hybrid basis sets (HF/6-311G* and MP2/6-311G*) as basis sets of choice for studying cisplatin's molecular properties.

Correspondence to: F. H. Hausheer

Presented in part at the 214th ACS National Meetings, Las Vegas, Nevada, September 7–11, 1997

We dedicate this work to the memory of Karen Wood

This article includes Supplementary Material available from the authors upon request or via the Internet at ftp.wiley.com/public/journals/jcc/suppmat/20/365 or http://journals.wiley.com/jcc/

© 1999 John Wiley & Sons, Inc.
CCC 0192-8651 / 99 / 030365-18

Furthermore, we recommend a hybrid ECP/HF approach with electron correlation for the most accurate physicochemical and electronic description of cisplatin and related compounds. © 1999 John Wiley & Sons, Inc. J Comput Chem 20: 365–382, 1999

Keywords: cisplatin; effective core potential; Hartree–Fock; Møller–Plesset correlation; anticancer drug

Introduction

Cis-diamminedichloroplatinum(II), cisplatin, (**1**) is one of the most important drugs for cancer treatment, and is effective in the treatment of cancers of the testis, ovary, head and neck, bladder, and lung.[1–3] Notwithstanding its broad clinical utility, cisplatin is a drug that has a relatively narrow therapeutic index and is associated with untoward side effects, including emesis, nephrotoxicity, myelosuppression, neurotoxicity, and other toxicities.[1s]

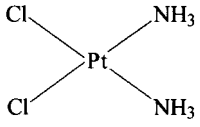

1

It has been postulated that the primary cytotoxic mechanism of tumor cell killing by cisplatin involves an initial displacement of one of the chlorines by a water molecule forming mono–aquo–mono–chloro–cisplatin inside the cell (**2**, Fig. 1). **2** is believed to be the major reactive cisplatin derivative that initially binds to one of the DNA

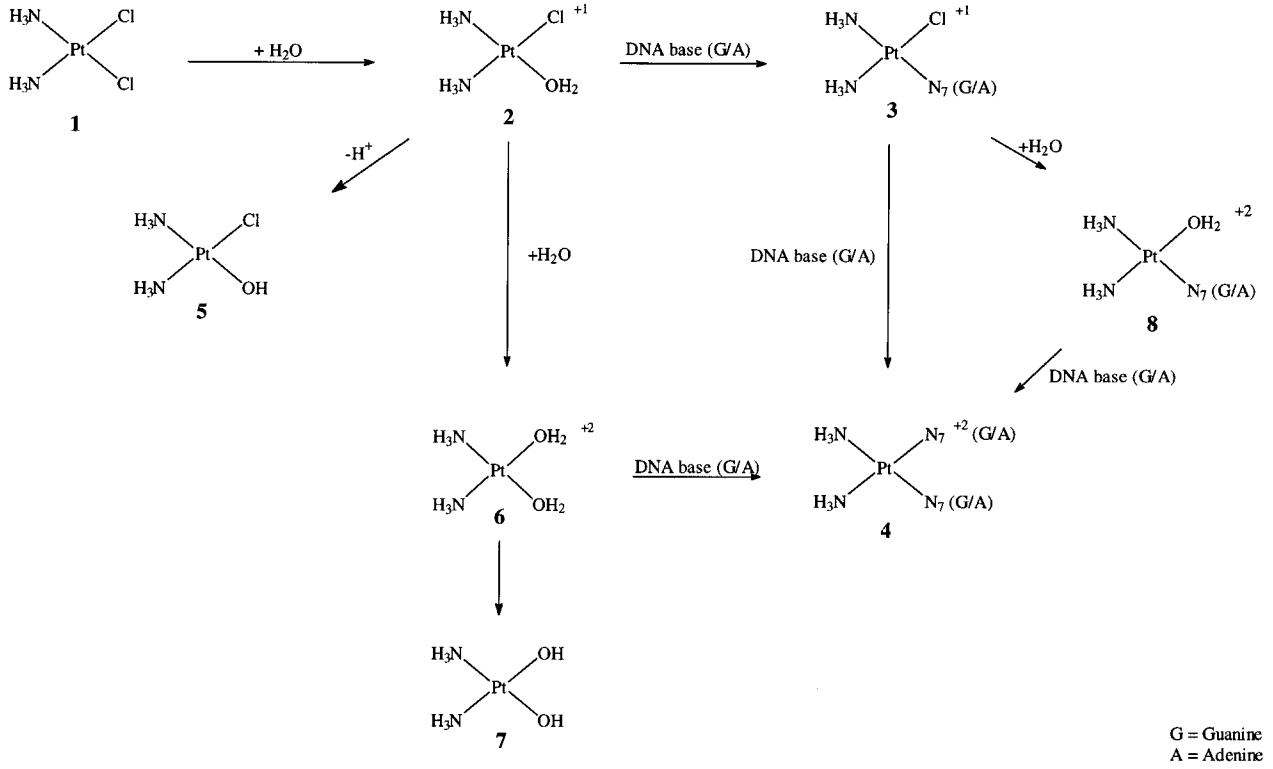

FIGURE 1. Postulated molecular species of cisplatin.

bases. The electron-rich N7 atom of the DNA bases, guanine (G) or adenine (A), is the primary bonding site of attack for **2** leading to **3**. Subsequent removal of the second chlorine atom from **3** by another water molecule leads to **8**. This mono–aquo–cisplatin derivative (**8**) subsequently attaches to the adjacent intrastrand N7 atom of G or A, finally forming **4**.[4] Binding of monoaquated cisplatin to the DNA bases is thought to occur largely in the form of intrastrand 1,2- or 1,3-DNA crosslinks; some investigators have postulated that interstrand[5] platinum–DNA crosslinks are also possible.

To obtain a mechanistic understanding of the key physicochemical properties of cisplatin, better structural information is needed for cisplatin and for hydroxy (**5**, **7**) and aquo derivatives (**2**, **6**) of cisplatin, along with detailed information on the interactions of cisplatin and its metabolites with DNA purines (**3**, **4**, and **8**). In the absence of extensive experimental data, including crystal structure information,[6,7] the geometries and electronic structures obtained from theoretical studies could provide valuable information to guide and complement these existing data. Until recently, more detailed theoretical studies of cisplatin could not be attempted because of the third row metal atom (Pt) involved, for which it is critical to address relativistic effects.[8] A variety of basis sets and pseudopotentials for third-row centers are now available and can be used to obtain better geometries and electronic structures for platinum species.[9]

There are only a few limited theoretical studies on cisplatin and its derivatives, and most of these studies are based on force-field calculations.[10] A recently published theoretical study on cisplatin (by Carloni et al.) used density functional theory (DFT) in the gradient-corrected local density approximation and their own pseudopotential scheme for platinum reported good agreement with the experimental bond lengths.[10a] A clear description of the bonding of cisplatin and optimized geometries, using a variety of high-quality *ab initio* basis sets along with the treatment for the electron correlation, has not been reported previously in the literature.

In part I of this series on the structure and bonding of cisplatin and its metabolites we present, for the first time, an extensive *ab initio* study on cisplatin, including electron correlation treatment up to the MP4 level. We also present the bonding in cisplatin from an *ab initio* quantum mechanical and a qualitative MO analysis using the fragment molecular orbital approach. This detailed and more comprehensive understanding of the performance of the theory and the identification of superior basis sets along with electron correlation methods will be helpful for future studies on the chemical, thermodynamic, and structural properties of cisplatin and related molecules.

Methodology

All calculations were performed using proprietary software[11], GAUSSIAN-94[12], and GAMESS[13] programs on the Cray T90, C90, J90, and EL98 class of supercomputers. Full geometry optimizations of cisplatin structures (with convergence criteria of maximum force of 0.00045 Hartree/Bohr, root-mean-square [RMS] force of 0.0003 Hartree/Bohr, maximum displacement of 0.0018 Bohr, and RMS displacement of 0.0012 Bohr) were carried out using gradient techniques.

We have employed a variety of basis sets for the ligands of cisplatin, NH_3 and Cl: 3-21G*,[14] 6-31G*,[15] 6-31G**, 6-311G*,[16] 6-311G**; including diffuse functions[17a] 6-31++G*, 6-311++G*; and including multiple d and p functions[17b] 6-311G(2d, 2p), 6-311++G(2d, 2p), 6-311++G(2d, 2pd), 6-311++G(3d, 3p), 6-311++G(3d, 3pd), D95,[18] and Dunning's correlation consistent valence double-zeta basis set along with polarization (cc-pVDZ).[19] Electron correlation treatment[20] was carried out at the MP2, MP3, and MP4 (SDQ) levels. Including the MP levels, a total of 30 basis sets were considered in the current study. We used six Cartesian d functions for polarization in all our calculations.

We employed two effective core potential (ECP) schemes for Pt: (1) ECP by Stevens, Basch, and Krauss (SBK[9a–c]); and (2) ECP from the Los Alamos Laboratory by Hay and Wadt (LanL2DZ).[9d–f] For the ECP of SBK, the Pt basis set was contracted as (7s/7p/5d)/[4111/4111/311], and in the ECP of LanL2DZ the basis set was contracted as (8s/6p/3d)/[341/321/21].

We considered three different conformations of cisplatin (**9**–**11**), two of them in C_{2v} symmetry (**9** and **10**) and one in C_s symmetry (**11**), and found that all are local minima on the potential energy surface. Because all three structures are degenerate in energy (using the HF/6-311G* basis set and using the ECP of SBK for Pt), we considered only structure **9** for subsequent analysis of cisplatin in this study. All MP calculations were done using the frozen core approximation.

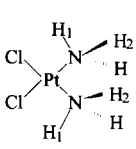

9, C_{2v}

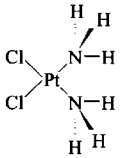

10, C_{2v}

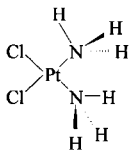

11, C_s

The quantum mechanically optimized structure of cisplatin (**9**) was verified by normal-mode frequency analysis at different levels: 6-31G*, 6-311G*, D95, MP2/D95, MP2/6-31G*, MP2/6-311G*, MP3/6-31G*, MP3/6-311G*, MP4(SDQ)/6-31G*, MP4(SDQ)/6-311G*, MP2/6-311++G(2d,2p), and MP2/6-311++G(2d, 2pd). All frequency calculations were performed using numerical second derivatives. We also verified that cisplatin structures **10** and **11** were local minima on the potential energy surface by normal-mode frequency analysis using the MP2/6-311G* and HF/6-311G* basis sets and obtained all positive eigenvectors for the Hessian for both basis sets.

The qualitative MO analyses were obtained by performing extended Hückel calculations[21] (using the program package Computer-Aided Composition of Atomic Orbitals, CACAO[22]) on the MP2/6-311G*-optimized geometry of cisplatin (**9**), and the interaction diagram was generated using the fragment molecular orbital (FMO) approach.[23] Parameters for all atoms used in the extended Hückel calculations were taken from the standard database in CACAO. The 2D contour diagrams of the MOs were also generated using CACAO. The molecular electrostatic potential (MEP) map was generated using the program ''mepmap'' (part of GAMESS). The charge density and the Laplacian of the charge density were generated using the atoms in molecules package (AIMPAC).[24]

Results

The *ab initio*–optimized total energies (a.u.) for cisplatin (**9**) using the ECP of SBK and LanL2DZ for Pt and a variety of basis sets on the ligands (NH_3 and Cl), including the electron correlation treatments, are given in Tables I (supplementary material) and II (supplementary material), respectively. The *ab initio*–optimized heavy atom geometric parameters for cisplatin using the ECP of SBK for Pt are given in Table III and the same parameters using the ECP of LanL2DZ for Pt are given in Table IV (supplementary material). Because we wanted to identify the overall per-

TABLE III.
***Ab Initio*–Optimized Geometric Parameters for Cisplatin (Using a Variety of Basis Sets on Ligands, NH_3 and Cl, and Using ECP of SBK Basis Set on Pt)**

Method	Pt—Cl	Δ_{c-o}	Pt—N	Δ_{c-o}	N—Pt—N	Δ_{c-o}	N—Pt—Cl	Δ_{c-o}	Cl—Pt—Cl	Δ_{c-o}	Overall[a] Mean Percent Difference
HF/3-21G*[b]	2.354	0.024	2.126	0.116	95.6	8.6	84.1	−6.2	96.2	4.3	5.6
HF/6-31G*	2.348	0.018	2.135	0.125	95.0	8.0	84.7	−5.6	95.6	3.7	5.3
HF/6-31G**	2.348	0.018	2.139	0.129	95.2	8.2	84.5	−5.8	95.7	3.8	5.4
HF/6-311G*	2.346	0.016	2.135	0.125	94.7	7.7	85.1	−5.2	95.1	3.2	5.0
HF/6-311G**	2.345	0.015	2.139	0.129	94.9	7.9	84.9	−5.4	95.3	3.4	5.2
HF/6-311++G*	2.345	0.015	2.132	0.122	94.7	7.7	84.9	−5.4	95.4	3.5	5.1
HF/6-311G(2d, 2p)	2.342	0.012	2.120	0.110	95.3	8.3	84.4	−5.9	95.9	4.0	5.3
HF/6-311++G(2d, 2p)	2.342	0.012	2.120	0.110	95.4	8.4	84.3	−6.0	96.0	4.1	5.4
HF/6-311++G(2d, 2pd)	2.343	0.013	2.117	0.107	95.4	8.4	84.3	−6.0	96.0	4.1	5.3
HF/6-311++G(3d, 3p)	2.343	0.013	2.118	0.108	95.6	8.6	84.2	−6.1	96.0	4.1	5.4
HF/6-311++G(3d, 3pd)	2.343	0.013	2.116	0.106	95.6	8.6	84.2	−6.1	96.0	4.1	5.4

TABLE III.
(continued)

Method	Pt—Cl	Δ_{c-o}	Pt—N	Δ_{c-o}	N—Pt—N	Δ_{c-o}	N—Pt—Cl	Δ_{c-o}	Cl—Pt—Cl	Δ_{c-o}	Overall[a] Mean Percent Difference
MP2 / 6-31G*	2.312	−0.018	2.090	0.080	97.1	10.1	84.2	−6.1	94.6	2.7	5.2
MP2 / 6-311G*[c]	2.307	−0.023	2.091	0.081	96.5	9.5	84.9	−5.4	93.8	1.9	4.8
MP2 / 6-311G*[d]	2.306	−0.024	2.091	0.081	96.6	9.6	84.8	−5.5	93.8	1.9	4.8
MP2 / 6-31++G*	2.312	−0.018	2.083	0.073	97.0	10.0	84.1	−6.2	94.8	2.9	5.2
MP2 / 6-311++G*	2.307	−0.023	2.084	0.074	96.8	9.8	84.5	−5.8	94.3	2.4	5.0
MP2 / 6-311G(2d, 2p)	2.310	−0.020	2.050	0.040	98.1	11.1	83.0	−7.3	95.8	3.9	5.6
MP2 / 6-311++G(2d, 2p)	2.311	−0.019	2.047	0.037	98.1	11.1	83.0	−7.3	95.9	4.0	5.6
MP2 / 6-311++G(2d, 2pd)	2.312	−0.018	2.034	0.024	98.2	11.2	82.8	−7.5	96.2	4.3	5.6
MP2 / 6-311++G(3d, 3p)	2.312	−0.018	2.041	0.031	98.4	11.4	82.8	−7.5	95.9	4.0	5.6
MP2 / 6-311++G(3d, 3pd)	2.312	−0.018	2.034	0.024	98.6	11.6	82.7	−7.6	96.0	4.1	5.6
MP3 / 6-31G*	2.327	−0.003	2.106	0.096	96.2	9.2	84.3	−6.0	95.2	3.3	5.2
MP3 / 6-311G*	2.324	−0.006	2.106	0.096	95.8	8.8	84.9	−5.4	94.4	2.5	4.8
MP4 / 6-31G*	2.326	−0.004	2.105	0.095	96.7	9.7	84.2	−6.1	94.8	2.9	5.2
MP4 / 6-311G*	2.320	−0.010	2.105	0.095	96.0	9.0	85.0	−5.3	94.0	2.1	4.7
All-SBK[e]	2.387	0.057	2.132	0.122	94.9	7.9	84.6	−5.7	95.9	4.0	5.6
MP2 / All-SBK	2.367	0.037	2.107	0.097	96.5	9.5	84.6	−5.7	94.2	2.3	5.2
HF / D95	2.393	0.063	2.135	0.125	95.4	8.4	83.9	−6.4	96.7	4.8	6.2
MP2 / D95	2.372	0.042	2.112	0.102	97.6	10.6	83.8	−6.5	94.9	3.0	5.9
HF / cc-pVDZ[f]	2.349	0.019	2.138	0.128	95.4	8.4	84.3	−6.0	95.9	4.0	5.6
Pt_SBK_others_LanL2DZ[g]	2.388	0.058	2.134	0.124	95.4	8.4	84.0	−6.3	96.7	4.8	6.1
DFT[h]	2.310	−0.020	2.060	0.050	98.0	11.0	83.0	−7.3	95.0	3.1	5.5
Expt (averaged)[i]	2.330	0.000	2.010	0.000	87.0	0.0	90.3	0.0	91.9	0.0	0.0
Expt (range)[i]	2.333, 2.328		1.950, 2.050		87.0 ± 1.5		92.0 ± 1, 88.5 ± 1		91.9 ± 0.3		

Distances in angstroms, angles in degrees. The "Δ_{c-o}" columns next to each geometric parameter correspond to the differences between the calculated value and the experimental value (calculated − observed). The last column refers to the percent difference obtained with respect to experimental values.

[a]For example, using HF / 3-21G*, the overall mean percent difference is calculated using absolute Δ_{c-o} as follows:

$$\left[\frac{0.024*100}{2.33}+\frac{0.116*100}{2.01}+\frac{8.6*100}{87.0}+\frac{6.2*100}{90.3}+\frac{4.3*100}{91.9}\right]*\frac{1}{5}=5.6.$$

[b]For example, the 3-21G* basis set was used on NH_3 and Cl and the ECP of SBK on Pt.

[c]Using MP2 with frozen core option.

[d]Using MP2 = full option.

[e]All atoms, including the ligand atoms (NH_3 and Cl) and platinum, were treated using the ECP of SBK.

[f]Dunning's correlation consistent-valence double-zeta with polarization basis set.

[g]Platinum atom was treated using the ECP of SBK and the ligand atoms were treated using the ECP of LanL2DZ.

[h]Ref. 10a.

[i]Ref. 6a.

formance of each basis set in comparison to the experimental geometric parameters of cisplatin, in Tables III and IV, we present the difference between the calculated and the observed values for all heavy-atom geometric parameters (''Δ_{c-o}'' column next to the various geometric parameters, e.g., Pt—Cl, Pt—N, etc.). The mean of all percentage differences for each basis set, defined as ''overall mean percent difference,'' is presented in the right-most columns of Tables III and IV.

BOND DISTANCES

Analysis of the heavy-atom bond distances data in Table III reveals several noteworthy observations: (a) When the basis set is smaller (3-21G*, 6-31G*), the cisplatin Pt—Cl and Pt—N bond lengths are longer than their experimental values with Δ_{c-o} much greater for the Pt—N bond length than for the Pt—Cl bond length. (b) As we increase the complexity of the basis sets on the ligands to 6-311G* or 6-311G(2d, 2p), the pattern for the Pt—N and the Pt—Cl bond lengths remains the same as above. (c) As we include electron correlation treatment at the MP2 level using the 6-31G* basis set on the ligands, the Pt—Cl bond length becomes shorter than the experimental value. The Pt—N bond length also becomes shortened compared with the value obtained using the aforementioned basis sets [6-311G* or 6-311G(2d, 2p)], but is still long compared with the experimental value. (d) As we increase the complexity of the basis set for the ligands to 6-311G*, 6-31++G*, 6-311++G*, 6-311G(2d, 2p), 6-311++G(2d, 2p), 6-311++G(2d, 2pd), 6-311++G(3d, 3p), and 6-311++G(3d, 3pd), while keeping the amount of correlation at MP2 level, the Pt—N bond length decreases. Furthermore, the Pt—Cl bond becomes shorter than the experimental value with all these basis sets. The Pt—N bond length comes very close to the observed value with either MP2/6-311++G(2d, 2pd) or MP2/6-311++G(3d, 3pd). (e) With the increase of correlation treatment to the MP3 and MP4 levels (using both 6-31G* and 6-311G* basis sets on the ligands), the Pt—Cl bond length remains close to the observed value, whereas the Δ_{c-o} for the Pt—N bond length at these basis sets increases.

From these observations we conclude that the Pt—Cl bond length is sensitive to the level of electron correlation employed, and is more properly described by a higher level of correlation treatment (e.g., MP3/6-31G* or MP4/6-31G*). On the other hand, the Pt—N bond length is more susceptible to changes in the basis set on the ligands [the larger the basis set, the better the agreement with the observed value, even at the MP2 level; viz., MP2/6-311++G(2d, 2pd)].

BOND ANGLES

The calculated N—Pt—N bond angle is as much as 8° to 9° higher than the experimental value using the smaller basis sets on the ligands, but as basis set complexity increases to HF/6-311G*, the value for this bond angle comes closer to the experimental value. Inclusion of electron correlation (at the MP2 level) increases this bond angle significantly compared with the experimental value.

On the other hand, the calculated N—Pt—Cl bond angles are smaller than the experimental value with all the basis sets. HF/6-311G*, MP4/6-311G*, MP2/6-311G*, HF/6-311G**, HF/6-311++G*, and MP3/6-311G* basis sets give the best estimate for this angle compared with the observed value. The calculated N—Pt—Cl angle was smallest and farthest from the experimental value with the MP2 basis sets.

The calculated bond angle for Cl—Pt—Cl showed the smallest deviation from experiment of the three bond angles considered. The application of the MP2/6-311G* basis set resulted in the smallest deviation from the experimental value.

Discussion

To identify the basis sets that can more accurately and precisely reproduce experimental bond lengths and bond angles, we compare the ''overall mean percent difference'' of all the calculated geometric parameters with respect to the observed values. Although the overall mean percent differences are within a narrow range for all the basis sets, the MP2/6-311G*, MP3/6-311G*, and MP4/6-311G* basis sets did the best in terms of giving the closest agreement with experiment. It is of interest to note that the HF/6-311G* basis set gave the next lowest (5.0) mean percentage difference. The results obtained with the density functional theory (DFT) for cisplatin[9a] were in notably good agreement in regard to bond lengths; however, because the DFT-calculated bond angles differ greatly from the experimental values, its mean percent difference is quite large (5.5).

These results lead us to conclude that, even if the ''overall mean percent difference'' is a convenient qualitative means for comparing basis set performance, because it is an all-inclusive quantity (average of calculated percent deviation of bond lengths and bond angles), one cannot read too much into this estimation alone.

It is clear that, as the complexity of the system increases, performing calculations involving electron correlation methods becomes prohibitively expensive; therefore, we recommend the HF/6-311G* basis set as a useful alternative for obtaining reasonable calculated geometries on larger systems.

CORE POTENTIAL APPROXIMATIONS

We also performed calculations on cisplatin using: (i) all-atom effective core potentials, employing the ECP of SBK for all the atoms; (ii) Dunning's basis set (D95); (iii) Dunning's basis set, including electron correlation (MP2/D95); (iv) Dunning's correlation consistent valence double-zeta with polarization basis set (cc-pVDZ) on the ligands and using the ECP of SBK for Pt; (v) using the ECP of SBK for Pt while treating other atoms using the LanL2DZ ECP basis set; and (vi) the same as (i), but including the electron correlation at the MP2 level. None of these basis sets were superior to the hybrid HF/MP results when compared with experimental values.

Comparing the results obtained using the ECP of SBK vs. LanL2DZ for Pt (Table III vs. Table IV), it can be seen that the Δ_{c-o} values for the Pt—Cl bond length were longer, whereas those for the Pt—N bond length were shorter with the LanL2DZ basis set. Increasing the level of electron correlation from MP2 did not improve the Δ_{c-o} for the Pt—Cl bond length. Increasing the complexity of the basis sets did improve Δ_{c-o} for the Pt—N bond length, as can be seen in Table III. Overall, we obtained a better agreement using the ECP of SBK for Pt rather than the ECP of LanL2DZ.

LIGAND (NH_3 AND Cl) GEOMETRIES

We also studied the performance of the theory with respect to calculated geometric parameters involving ligand atoms (NH_3 and Cl); viz., N—H bond lengths and Pt—N—H_1 and Pt—N—H_2 bond angles (Table V, supplementary material). Table V also lists certain nonbonded distances for Cl $\cdots$ H_1, Pt $\cdots$ H_1, and N $\cdots$ Cl. In the original crystal structure report on cisplatin, Milburn et al.[6a] concluded that the same chlorine atom from a second molecule in the unit cell has favorable interactions with the in-plane hydrogens from both NH_3 groups of the first molecule (intermolecular interaction). These investigators and the earlier work by Chatt[25] also hypothesized certain molecular orbital interactions between Pt and the in-plane hydrogen from the NH_3 of the same molecule. We also noticed that, in the original crystal structure of cisplatin,[6a] the intramolecular N $\cdots$ Cl nonbonded distance between the adjacent NH_3 and the chlorines was 3.01 Å, which is within the hydrogen-bond distance for N—H $\cdots$ Cl (3.00–3.20 Å).[26]

The calculated intramolecular N $\cdots$ Cl nonbonded distance is found to be in the range of 2.88 to 3.05 Å (Table V, using the ECP of SBK for Pt), indicating a possible hydrogen bond between N—H_1 $\cdots$ Cl. Also, the Cl $\cdots$ H_1 distance is found to be in the range of 2.33 to 2.57 Å, thus in the range of forming a hydrogen-bond interaction between Cl and H_1. Due to the symmetry (C_{2v}), we find an identical distance between the in-plane hydrogen from the second NH_3 and the second Cl atom.

As mentioned elsewhere in regard to a possible Pt $\cdots$ H_1 nonbonded interaction,[6a] the calculated Pt $\cdots$ H_1 nonbonded distance was also short (2.45 to 2.57 Å). We examine the nature of this interaction further in the next subsection.

The N—H_1 (in-plane) bond lengths are calculated to be 1.02 Å and those involving out-of-plane hydrogens are 1.01 Å at the MP2/6-311G* level. The Pt—N—H_1 (in-plane hydrogen) angle was smaller (101° to 105°) than the other two involving the out-of-plane hydrogens (113° to 115°) to accommodate the N—H $\cdots$ Cl interactions.

Table VI (supplementary material) presents similar geometric parameters, as discussed in Table V, but using the ECP of LanL2DZ for Pt, and, as expected, the trends are similar to those in Table V.

BONDING IN CISPLATIN: QUALITATIVE MO ANALYSIS

To understand the nature of the bonding interactions that provide stability in the molecular system, and to explain some of the key intramolecular interactions noted earlier (i.e., intramolecular N—H $\cdots$ Cl hydrogen-bond and Pt $\cdots$ H nonbond interactions), we need a detailed description of the various orbitals responsible for the bonding. In this subsection, we present a qualitative molecular or-

bital analysis of cisplatin based on the fragment molecular orbital (FMO) approach within extended Hückel formalism.

Using the FMO approach, we constructed the interaction diagram for cisplatin by interacting the fragment orbitals of Pt^{2+} and $[(NH_3)_2 \cdots Cl_2]^{2-}$ (Fig. 2). The extended Hückel energy levels for the fragments and cisplatin were obtained by using the MP2/6-311G*-optimized geometry of cisplatin. The five degenerate d-orbital energy levels of Pt^{2+} are shown on the right side of Figure 2. Because Pt is in the +2 state (d^8), only four of the five degenerate MOs are occupied. These are $d_{x^2-y^2}$ ($2a_1$), d_{z^2} ($1a_1$), d_{xy} ($1a_2$), and d_{xz} ($1b_1$), based on the coordinate system shown in Figure 2. The symmetry labels are based on the C_{2v} symmetry. The d_{yz} ($1b_2$) orbital on Pt becomes the lowest unoccupied MO (LUMO). The fragment orbital

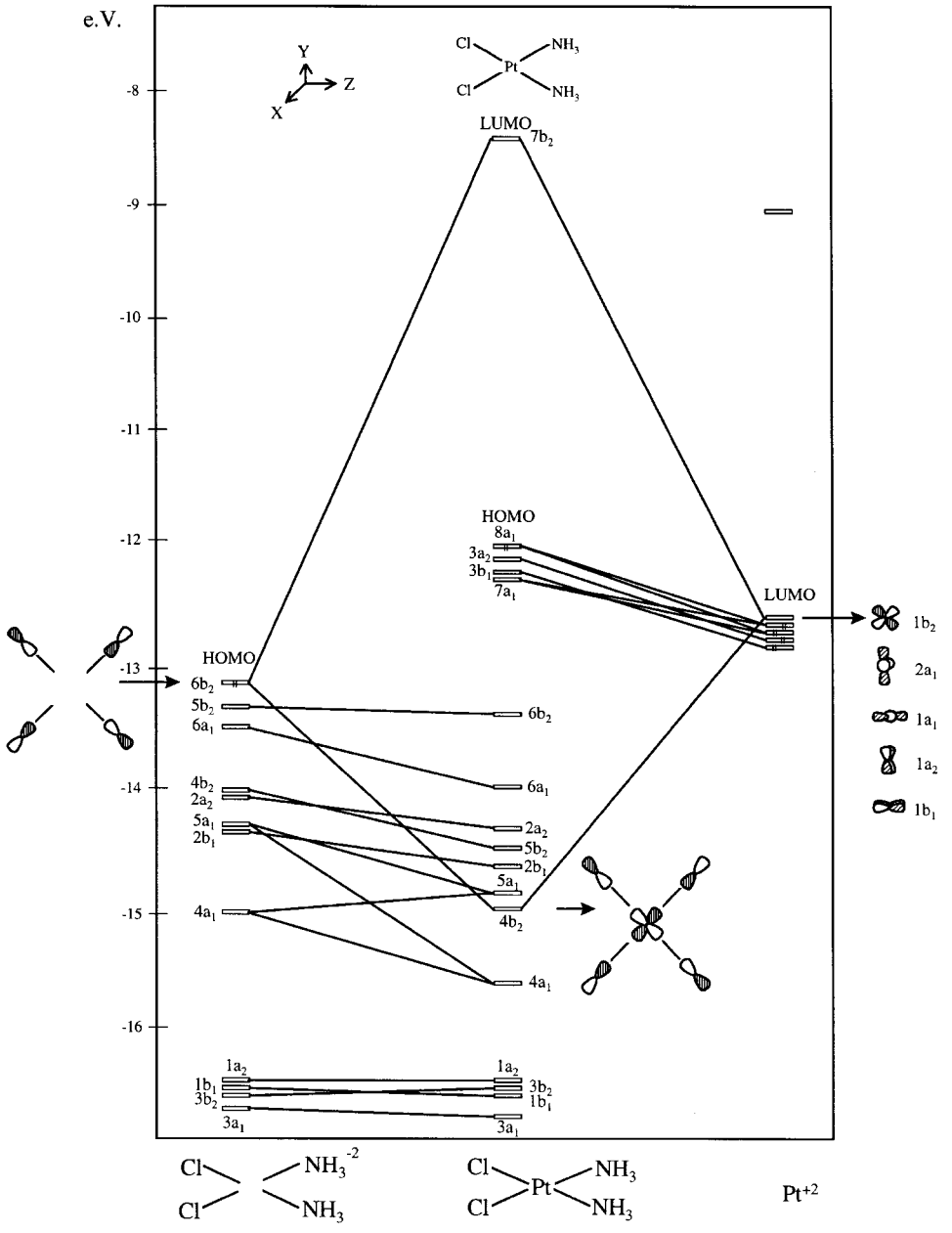

FIGURE 2. Interaction diagram showing how the orbitals of $[(NH_3)_2 \cdots Cl_2]^{2-}$ (left side) and Pt^{2+} (right side) interact to give the orbitals of $Pt(NH_3)_2Cl_2$ (middle). The five d orbitals for Pt^{2+} shown on the right side of the figure are degenerate in energy.

energy levels of the ligand $[(NH_3)_2 \cdots Cl_2]$ are shown on the left side of Figure 2 and the orbital energy levels of cisplatin are shown in the middle of Figure 2.

As the five energetically degenerate orbitals of platinum start interacting with the fragment orbitals of the ligand, they split into five MOs, with the four occupied MOs clustered together in a narrow energy range. All four MOs are slightly destabilized by antibonding interaction with the fragment orbitals of $[(NH_3)_2 \cdots Cl_2]$. These are the HOMO $8a_1$ ($d_{y^2-z^2}$), $3a_2$ (d_{xy}), $3b_1$ (d_{xz}), and $7a_1$ ($d_{z^2-x^2}$), and are shown in the following structures. The atom labels for the MOs are based on the structure of cisplatin.

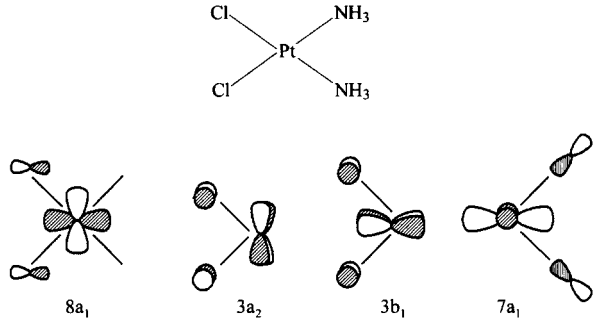

In both $8a_1$ and $7a_1$, the platinum d orbitals are obtained as a result of the mixing between the $d_{x^2-y^2}$ and d_{z^2} orbitals on Pt interacting in an antibonding manner with the chlorine (p_z orbital) and the hybrid "p" (p_y and p_z orbitals) from the nitrogen (NH_3), respectively. In $3a_2$, the d_{xy} orbital on Pt interacts in an antibonding way (δ^* type) with the chlorine p_x orbitals. In $3b_1$, the d_{xz} orbital on Pt interacts in an antibonding way (π^* type) with the chlorine p_x orbitals. The corresponding bonding orbitals are composed mainly of the ligand $[(NH_3)_2 \cdots Cl_2]$ MOs. These are $6a_1$, $2a_2$, $2b_1$, and $5a_1$ and are as shown.

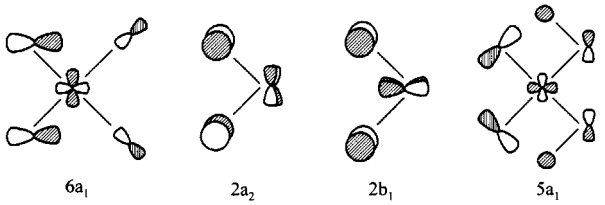

In $2a_2$, the p_x orbitals on the chlorines interact in a bonding manner (δ type) with the d_{xy} orbitals on Pt. In this MO, the p_x orbitals on the chlorines correspond to the antibonding combination of the out-of-plane lone pairs. In $2b_1$, the p_x orbitals on the chlorines interact in a π-bonding manner with the d_{xz} orbital on Pt. Here, the combination of the two p_x orbitals on the chlorines represents the bonding combination of the out-of-plane lone pairs.

$6a_1$ has the $d_{z^2-y^2}$ orbital on platinum interacting in a bonding manner with the p_z orbitals on the chlorine and the hybrid p orbital (p_z and p_y) from the nitrogen (NH_3). In $5a_1$, the $d_{y^2-z^2}$ orbital of platinum interacts in a bonding manner with the hybrid p orbital (p_y and p_z) on the chlorines and the p_y orbital on the nitrogen (NH_3). The p orbitals on the chlorines in this MO represent the bonding combination of the in-plane lone pairs on the chlorines.

The one MO that showed significant stabilization by the interaction of the fragment orbitals is $4b_2$, which is obtained by a bonding interaction between the d_{yz} (LUMO) orbital of Pt with the ligand (NH_3 and Cl) p_y and p_z orbitals. d_{yz} is a two-electron/two-orbital interaction that gives stability to the molecule. The corresponding antibonding orbital greatly increases in energy and becomes the LUMO of cisplatin ($7b_2$). These two orbitals are shown graphically, and contour diagrams of these two MOs are shown in Figure 3 ($7b_2$ and $4b_2$).

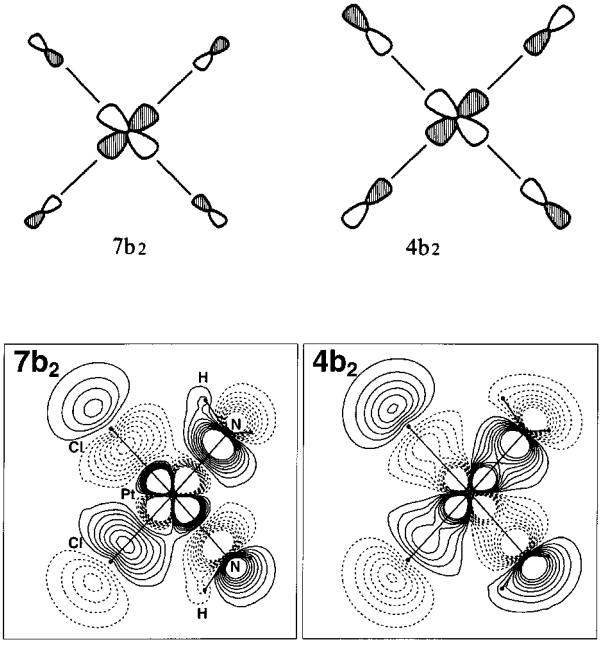

FIGURE 3. Two-dimensional contour diagrams of the orbitals $7b_2$ and $4b_2$ obtained using the extended Hückel wave function. The contour values start at 0.015 with increments of 0.015.

MO $6b_2$ does not have any contribution from the metal AOs, and thereby remains stationary in its energy. The p orbitals on the chlorines in this MO represent the antibonding combination of the in-plane lone pairs on the chlorines.

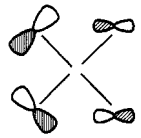

$6b_2$

Two other MOs ($5b_2$ and $4a_1$) show stabilization and a drop in energy. In both these MOs, platinum orbitals (p_y and $d_{x^2-z^2}$, respectively) interact in a bonding manner with the p orbitals on the chlorine and the nitrogen of NH_3. These two MOs are shown.

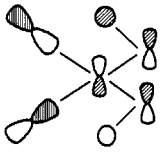

$5b_2$

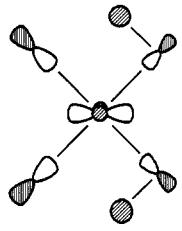

$4a_1$

NATURE OF Pt···H AND N—H···Cl INTERACTIONS

To determine if there is any interaction between Pt and the in-plane hydrogens from NH_3, we first look at the Mulliken overlap population between the two atoms. This was found to be -0.05 electron (at the *ab initio*–optimized geometry of cisplatin using the MP2/6-311G* basis set and the ECP of SBK for Pt, antibonding) and could be traced to the $5b_2$ and $5a_1$ orbitals where Pt interacts in an antibonding way with the in-plane hydrogens of NH_3. Casas et al. noted that, when the Pt···H nonbonded distance is > 2.5 Å, it would lead to an antibonding interaction between the two atoms.[27] Contour diagrams of these two MOs are shown in Figure 4 ($5b_2$ and $5a_1$ supplementary material).

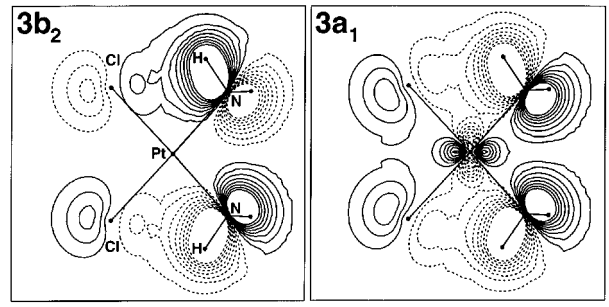

FIGURE 5. Two-dimensional contour diagrams of the $3b_2$ and $3a_1$ orbitals obtained using the extended Hückel wave function. The contour values start at 0.015 with increments of 0.015. In the $3a_1$ orbital, the in-plane hydrogen from the NH_3 overlaps (in a bonding way) with the chlorine atom only. The contour plot of the same MO containing contributions from Pt and the in-plane hydrogen clearly indicates that there is no overlap between the two atoms (plot not shown).

Concerning the N—H···Cl intramolecular hydrogen bonding, $3a_1$ and $3b_2$ MOs have bonding interactions between chlorine and the in-plane hydrogen of the NH_3 group. Contour diagrams of $3b_2$ and $3a_1$ MOs are shown in Figure 5 . Overall, the Mulliken overlap population indicates a bonding interaction between Cl and the in-plane hydrogen from the NH_3 groups, the value being $+0.05$ electron, again at the same basis set as expressed earlier.

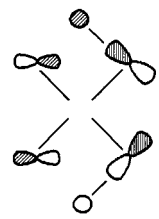

$3b_2$

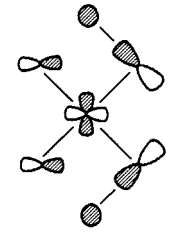

$3a_1$

VIBRATIONAL ANALYSIS OF CISPLATIN

We were interested in determining the performance of the theory by calculating the vibrational frequencies of cisplatin and comparing them with the experimental values.[28] This comparison provides an indication of how well our calculated structure of cisplatin can reproduce the IR spectrum. A calculated structure of cisplatin that ac-

curately reproduces its experimental vibrational spectrum is a more rigorous test of the basis set performance as applied to the description of structural and thermodynamic properties relative to an x-ray-determined geometry, which can be affected by crystal packing, intermolecular interactions, etc.

We undertook a detailed normal-mode frequency analysis on cisplatin (C_{2v} geometry, **9**) using various basis sets on the ligands, including 6-31G*, 6-311G*, D95, MP2/D95, MP2/6-31G*, MP2/6-311G*, MP3/6-31G*, MP3/6-311G*, MP4 (SDQ)/6-31G*, MP4 (SDQ)/6-311G*, MP2/6-311++G(2d, 2p), and MP2/6-311++G(2d, 2pd), using the ECP of SBK on Pt, and using the respective optimized geometry for each basis set. For all basis sets, the C_{2v} geometry (**9**) is found to have all positive eigenvectors for the Hessian, which indicates that the calculated structure of cisplatin is a local minimum on the potential energy surface.

In Table VII we compare the calculated vibrational frequencies with the experimental values. Of the 27 vibrational modes that are possible for cisplatin, 9 belong to a_1 symmetry, 5 to a_2 symmetry, 5 to b_1 symmetry, and 8 to b_2 symmetry. The vibrational modes belonging to the a_2 symmetry are not IR active.

Pt—N AND Pt—Cl STRETCH

Earlier infrared (IR) studies on cisplatin identified the vibrational frequencies corresponding to the Pt—Cl, Pt—N, and N—H stretching modes, and also identified the deformation modes like rocking, symmetric, and degenerate vibrations of NH_3.[28] All these spectra indicate strong absorption for the $\delta(NH_3)$ symmetric and rocking deformation and N—H stretching vibration.

In Table VII, the calculated Pt—Cl stretching frequencies are close to the experimental values for all basis sets (within 5.0–13.9%). On the other hand, the calculated Pt—N stretching frequency shows a wide variation (0.6–17.7%), with all basis sets, and is closest to the observed value[28a] (508 and 517 cm^{-1}) when using the MP2/6-311++G(2d, 2pd) basis set (505 and 511 cm^{-1}). This can be explained based on the fact that our calculated Pt—N bond length was very close to the experimental value using the MP2/6-311++G(2d, 2pd) basis set, and was longer for all other basis sets.

The calculated IR spectrum of cisplatin using the MP2/6-311++G(2d, 2pd) basis set on the ligands, and using the ECP of SBK on Pt, is presented in Figure 6b; Figure 6a shows a redrawn experimental IR spectrum of cisplatin[28a] for comparison purposes.

DEFORMATION MODES OF $\delta(NH_3)$: DEGENERATE, SYMMETRIC, AND ROCKING

As seen from the experimental spectra of cisplatin,[28] we also see three regions in the calculated IR spectrum of cisplatin [at MP2/6-311++G(2d, 2pd) basis set and using the ECP of SBK for Pt] corresponding to the deformation vibrations of the NH_3 ligand. These are the $\delta(NH_3$, degenerate), $\delta(NH_3$, symmetric), and $\delta(NH_3$, rocking) regions (Fig. 6b). As indicated in Figure 6b, $\delta(NH_3$, degenerate) split into three bands and the magnitude of the splitting is 40 cm^{-1} (1632, 1644, and 1672 cm^{-1}). The band corresponding to the frequency of 1644 cm^{-1} is weak. The experimental frequencies for this deformation are found to be in the range of 1544–1625[28a] cm^{-1} (two bands found experimentally, Fig. 6b). In another experimental determination of IR spectrum on cisplatin, Mizushima et al.[28b] found three bands for this deformation and one of them is a weak one, similar to what we found in our calculated spectrum.

To explain the splitting in this region, Chatt et al.[25] hypothesized interactions between the d orbitals on Pt and the in-plane hydrogens on the NH_3 ligand. However, according to our calculations, $Pt \cdots H_1$ nonbonded interactions are found to be antibonding. The presence of $N—H_1 \cdots Cl$ hydrogen-bond interactions are probably more responsible for the kind of splitting observed for the degenerate deformations of NH_3.

We also observed a splitting in the calculated spectrum in the region of 1300 cm^{-1} (1294 and 1303), corresponding to the $\delta(NH_3)$ symmetric deformation vibration as seen in the experimental spectra. Again, as seen from the experimental[28a] splitting in this region (1301 and 1316 cm^{-1}, magnitude of splitting is 15 cm^{-1}), our calculated splitting for the symmetric deformation vibration is also small (9 cm^{-1}).

We observed four frequencies in the range 725–790 cm^{-1}, with the frequency at 791 cm^{-1} having the greatest intensity. This frequency is close to the observed $\delta(NH_3)$ rocking vibration as found in the experimental spectrum (795 cm^{-1}).[28a] Of the remaining three, one is IR inactive and the other two are very weak compared with that at 791 cm^{-1}.

TABLE VII.

Calculated Normal-Mode Frequencies of Cisplatin Using a Variety of Basis Sets on Ligands (NH_3 and Cl) Including HF / 6-31G*, HF / 6-311G*, D95, MP2 / D95, MP2 / 6-31G*, MP2 / 6-311G*, MP3 / 6-31G*, MP3 / 6-311G*, MP4 (SDQ) / 6-31G*, MP4 (SDQ) / 6-311G*, and MP2 / 6-311 + + G(2d, 2pd), and Using ECP of SBK for Pt. Experimentally Obtained Vibrational Frequencies Also Included for Comparison (All Frequencies in cm^{-1}).

Symmetry of the Mode	Mode #	Type of Mode	Calculated Frequencies at: HF / 6-31G*	HF / 6-311G*	D95	MP2 / [a] D95	MP2 / [a] 6-31G*	MP2 / [a] 6-311G*	MP3 / [a] 6-31G*	MP3 / [a] 6-311G*	MP4 / [a] 6-31G*	MP4 / [a] 6-311G*	MP2 / [a] 6-311 + + G(2d, 2pd)	Expt.[b]
a_1	ν7	N—Pt—N *bend*	227	225	232	224	223	216	222	216	221	214	233	222
		Intensity	(20)	(19)	(19)	(24)	(25)	(24)	(23)	(22)	(23)	(22)	(34)	
b_2	ν8	Pt—Cl *str*	336	336	333	350	361	360	353	352	353	354	357	317
		Intensity	(50)	(51)	(47)	(35)	(35)	(36)	(38)	(40)	(35)	(36)	(36)	
a_1	ν9	Pt—Cl *str*	348	348	344	358	369	369	362	362	362	362	368	324
		Intensity	(42)	(43)	(40)	(27)	(28)	(28)	(30)	(31)	(28)	(29)	(26)	
b_2	ν10	Pt—N *str*	419	418	439	475	466	464	452	450	453	450	505	508
		Intensity	(8)	(9)	(12)	(11)	(6)	(7)	(6)	(8)	(7)	(8)	(5)	
a_1	ν11	Pt—N *str*	435	432	451	480	474	469	462	458	462	457	511	517
		Intensity	(3)	(3)	(6)	(4)	(3)	(3)	(3)	(3)	(3)	(3)	(0.1)	
a_1	ν15	δNH_3 *rock*	845	841	888	842	832	814	825	812	827	812	791	795
		Intensity	(95)	(94)	(100)	(80)	(77)	(76)	(84)	(84)	(76)	(73)	(78)	
b_2	ν16	δNH_3 *symm*	1452	1453	1441	1341	1353	1357	1373	1382	1366	1374	1294	1301
		Intensity	(249)	(220)	(392)	(254)	(174)	(161)	(199)	(182)	(173)	(153)	(139)	
a_1	ν17	δNH_3 *symm*	1461	1462	1452	1349	1362	1367	1382	1391	1375	1383	1303	1316
		Intensity	(162)	(156)	(269)	(150)	(100)	(101)	(121)	(120)	(99)	(98)	(108)	
b_2	ν18	δNH_3 *deg*	1818	1833	1824	1694	1697	1700	1710	1716	1703	1709	1632	1544
		Intensity	(39)	(37)	(49)	(47)	(43)	(41)	(40)	(38)	(40)	(39)	(28)	
b_1	ν21	δNH_3 *deg*	1852	1869	1862	1727	1731	1735	1745	1752	1737	1743	1672	1625
		Intensity	(66)	(65)	(91)	(62)	(53)	(54)	(56)	(56)	(52)	(52)	(28)	
b_2	ν22	N—H *str*	3674	3712	3651	3380	3439	3484	3480	3530	3440	3486	3434	3232
		Intensity	(55)	(37)	(44)	(22)	(41)	(25)	(41)	(27)	(29)	(16)	(24)	
a_1	ν25	N—H *str*	3791	3813	3794	3531	3570	3606	3593	3632	3556	3592	3586	—
		Intensity	(91)	(67)	(103)	(74)	(92)	(70)	(79)	(60)	(69)	(50)	(80)	

str, stretching vibration; *rock*, rocking vibration of NH_3; *symm*, symmetric deformation vibration of NH_3; *deg*, degenerate deformation vibration of NH_3; *bend*, skeletal bending vibration.

[a] Using the frozen core MP2 calculations.

[b] Ref. 28a.

N—H STRETCHING

We observed six frequencies corresponding to the N—H stretching vibrational mode, one of which is IR inactive. Two of the calculated N—H stretching frequencies are 3434.2 (weak) and 3434.4 (strong) cm^{-1} and are larger compared with experimental values (3232 and 3297 cm^{-1}),[28a] which is due in part to the shorter calculated N—H bonds and also to the slightly longer Pt—N bonds, which strengthen the N—H stretching frequencies.[28e] The other three frequencies are calculated to be at 3585 (weak), 3586 (strong), and 3647 (strong) cm^{-1}, whereas the experimental spectrum did not show frequencies in this region.

The calculated frequencies in the range 150–260 cm^{-1} are assigned to the skeletal bending

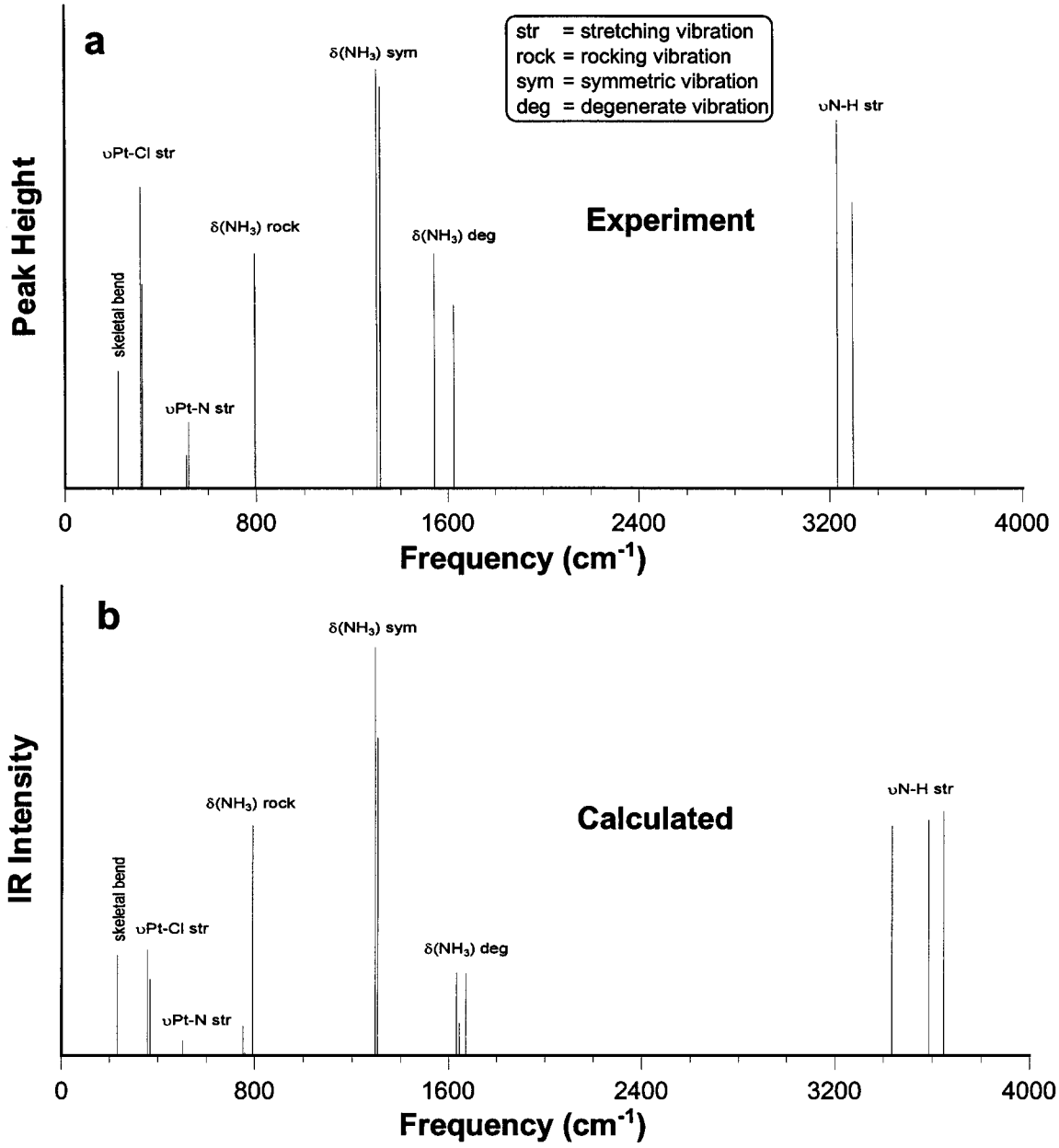

FIGURE 6. Comparison of experimental (a) and calculated (b) IR spectra of cisplatin. The experimental spectrum was redrawn from ref. 28a and the peak heights were measured relative to the same baseline. The calculated spectrum was obtained using the MP2/6-311++G(2d, 2pd) basis set on the ligands of cisplatin and using the ECP of SBK on Pt.

of cisplatin, viz., N—Pt—N, Cl—Pt—Cl, and N—Pt—Cl bending vibrations.

Based on the previous analysis, the calculated IR spectrum shown in Figure 6b matches with the experimental spectrum (Fig. 6a) with respect to the various vibrational modes. These results support our calculated spectrum. As a note of caution, one should not overlook the fact that we are comparing the gas-phase-calculated frequencies with the experimentally determined IR spectrum, which was carried out at room temperature.

We also performed the frequency calculations using all basis sets mentioned earlier on the ligands and using the ECP of LanL2DZ on Pt. Because the trends are similar to those observed in Table VII, we do not present them here.

MOLECULAR ELECTROSTATIC POTENTIAL

To characterize the sites of attack on cisplatin for any incoming nucleophile or electrophile, it is helpful to study the molecular electrostatic potential (MEP) around the cisplatin molecule. We calculated the MEP for cisplatin using the *ab initio*–optimized geometry at the MP2/6-311G* level and using the ECP of SBK for Pt, and the MEP is presented in Figure 7a and b. We find three minima in the potential surface in the plane shown in Figure 7a. One minimum is at −35.2 kcal/mol, designated **II** in Figure 7a, and is 1.824 Å away from one of the chlorines, making an angle of 142.3° with the platinum. Due to the symmetry, we see an identical minimum on the second chlorine (designated as **II** in Fig. 7a). The third minimum at −63.3 kcal/mol (designated as **I** in Fig. 7a) is 2.052 Å away from both the chlorines making an angle of 78.0° with the platinum.

We found two more minima in the potential surface on each chlorine in a plane perpendicular to the one used in Figure 7a and is shown in Figure 7b. Each has a value of −49.5 kcal/mol and is 1.650 Å away from the chlorine making an angle of 114.9° with the platinum (designated **III** in Fig. 7b). As seen from our (FMO) qualitative analysis, these minima around the chlorines correspond to the lone pair of electrons representing the p orbitals.

The calculated electrostatic potential (ESP) charges at the HF/6-311G* and MP2/6-311G* basis sets are shown in Table VIII (supplementary material). The chlorines have a more negative charge (−0.342 at MP2/6-311G*) than the platinum (−0.052 at MP2/6-311G*). The potential around the ammines is positive (charge on N is

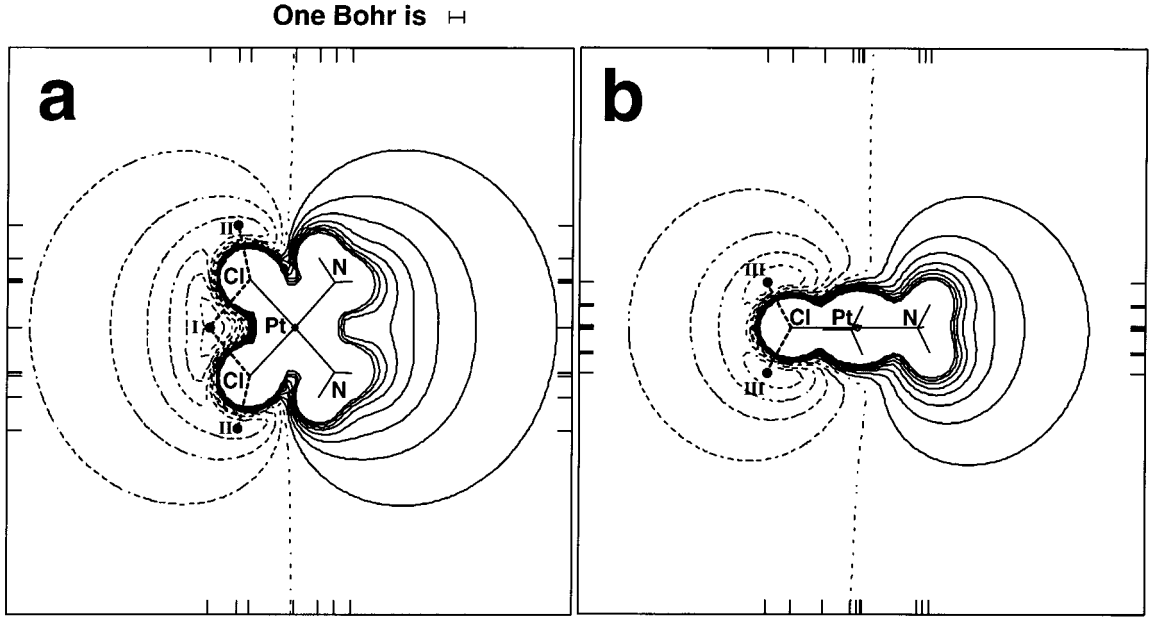

FIGURE 7. Two-dimensional contour drawings of the molecular electrostatic potential (MEP) of cisplatin obtained using GAMESS with the MP2/6-311G* basis set and using the ECP of SBK on Pt. (a) Molecule in the *XY* plane. (b) Molecule in the *YZ* plane. The filled circles with Roman numerals indicate the locations of the minima in the potential around the chlorine atoms.

-0.424, and each hydrogen has a charge of $+0.264$ at MP2/6-311G*) as indicated by the solid lines in Figure 7.

CHARGE DENSITY AND LAPLACIAN OF CHARGE DENSITY

So far, our discussion on the bonding of cisplatin centered around using the molecular orbital concepts. Bader et al.[24] proposed another way of studying chemical bonding by using the charge density, $\rho(r)$, which is obtained directly from the wave function. In this approach, the topology of $\rho(r)$ identifies chemical components such as atoms, bonds between pairs of atoms, and structure. The topology of the charge density is characterized by a set of critical points that are found on all nuclei and between every pair of bonded atoms with a covalent bond.[29] Using this approach, it is also possible to locate certain weak interactions, such as hydrogen bonds.[30] The only caveat to this is, if the electron density in the region of the hydrogen bond is not sufficient or if the minimizer that locates the critical points is not robust, then finding the location of the critical point in such a region will be more difficult.

The calculation of the Laplacian of the charge density [$\nabla^2\rho(r)$] provides further supportive information. A value of $\nabla^2\rho(r) < 0$ (charge accumulation) at a bond critical point is related to a covalent bond. When $\nabla^2\rho(r) > 0$, it indicates charge depletion. However, $\nabla^2\rho(r)$ is expected to be greater than zero for ionic bonds, hydrogen bonds, and van der Waals molecules.

We used the wave function obtained from the *ab initio*–optimized geometry of cisplatin using the MP2/6-311++G(2d, 2pd) basis set and using ECP of SBK for Pt to obtain the charge density, $\rho(r)$, and the Laplacian of the charge density, $\nabla^2\rho(r)$. Contour drawings of these two quantities are presented in Figure 8a and b, respectively. As expected, we found nuclear critical points on all the nuclei and bond critical points between Pt—N, Pt—Cl, and N—H atoms (Fig. 8a). The bond critical points are indicated in Figure 8a by numerals **1** (for the Pt—Cl bond), **2** (for the Pt—N bond), and **3** (for N—H bond). However, we could not locate the bond critical point between $Cl\cdots H_1$ for the $N—H\cdots Cl$ hydrogen bond, even though the contour lines have the expected shape as seen for the other hydrogen bonds ($C—H\cdots O$[31]), indicating an interaction between $Cl\cdots H_1$. As mentioned

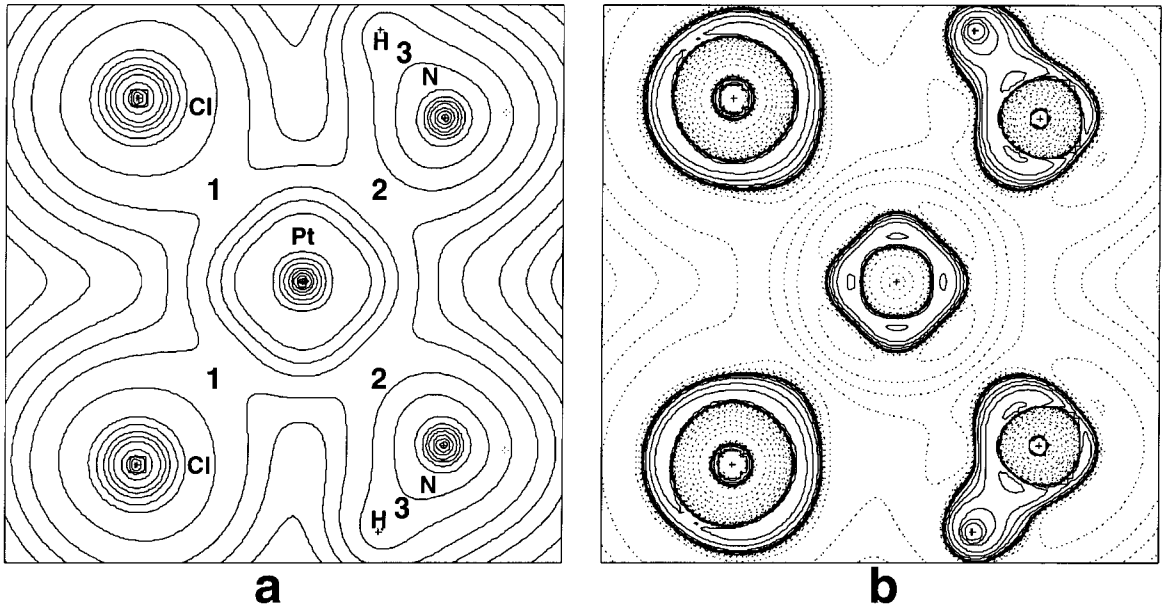

FIGURE 8. Two-dimensional contour drawings of charge density, $\rho(r)$ (a), and the Laplacian of the charge density, $\nabla^2\rho(r)$ (b), of cisplatin obtained using the MP2/6-311++G(2d, 2pd) basis set and using the ECP of SBK on Pt using the AIMPAC program. In (a), the numbers indicate the positions of the bond critical points in cisplatin: **1** is the bond critical point for the Pt—Cl bond; **2** is the bond critical point for the Pt—N bond; and **3** is the N—H bond critical point. On each nucleus, we have the nuclear critical point. In (b), for the Laplacian of the charge density, negative-value contours are represented by solid lines and positive-value contours by dashed lines.

previously, either the charge density in this region was low or the minimizer was not able to locate the critical point indicating the hydrogen bond between Cl and H_1.

The Laplacian of the charge density (Fig. 8b) clearly shows a negative charge [$\nabla^2\rho(r) < 0$] between Pt—N, Pt—Cl, and N—H bonds, indicating that there is charge accumulation and bond formation between these atoms.

Conclusions

We have presented the first extensive theoretical study using an *ab initio* approach on cisplatin using both pure effective core potential (ECP) and a variety of hybrid HF/ECP basis sets (on the ligands, NH_3 and Cl) and ECPs on Pt (SBK and LanL2DZ), and have also included electron correlation treatments up to the MP4 level. These results were compared with other available theoretical results and experimental geometries and were found to be in good agreement with experimental geometries and properties. The results suggest some of the basis sets that can be used when the complexes of cisplatin with other molecular targets are considered. The two best basis sets were shown to be HF/6-311G* and MP2/6-311G*, depending on computer resources and the size of the molecular system. The best overall performance was observed with the MP2/6-311G* basis set, whereas the HF/6-311G* basis set gave good agreement and is more economical.

The calculated vibrational frequencies for the Pt—Cl and the Pt—N stretching modes compare very well with the experimental values as do the deformation vibrational modes of the NH_3 ligand (degenerate, symmetric, and rocking). In this study, we have also presented molecular electrostatic potential (MEP) and the electrostatic potential (ESP) charges for prediction of sites of attack on cisplatin.

The qualitative MO analysis explains the bonding in cisplatin and certain intramolecular interactions between Cl $\cdots$ H and between Pt $\cdots$ H. Based on our analysis, the chlorines have intramolecular hydrogen-bond interactions with the in-plane hydrogens of the ammine groups. The nonbonded interaction between Pt and H was found to be antibonding. The bonding in cisplatin was also presented using the charge density and the Laplacian of the charge density. Further results on the structure and properties of cisplatin complexes will be presented in the future.

Supplementary Material

Tables of the calculated energies (Tables I and II), ligand geometries (Tables IV, V, and VI), electrostatic potential charges (Table VIII), and Figure 4 for cisplatin are available as supplementary material from the *Journal of Computational Chemistry*.

Acknowledgment

We thank Suzi Lozano for help in preparing the manuscript and Sandra Peter for the expert rendering of the drawings. We thank SGI/Cray Research for the computer time on C90 and T90 supercomputers. We also thank the referees for their many helpful comments and suggestions.

References

1. (a) Reedijk, J.; Fichtinger-Schepman, A.M. J.; van Oosterom, A. T.; van de Putte, P. Struct Bonding (Berl) 1987, 67, 53. (b) Bruhn, S. L.; Toney, J. H.; Lippard, S. J. Prog Inorg Chem 1990, 38, 477. (c) Farrell, N. In: James, B. R.; Ugo, R., eds. Catalysis by Metal Complexes. Reidel-Kluwer: Dordrecht, 1989, The Netherlands, pp 46–66. (d) Sherman, S. E.; Lippard, S. J. Chem Rev 1987, 87, 1153. (e) Rosenberg, B.; van Camp, L.; Trosko, J. E.; Mansour, V. H. Nature 1969, 222, 385. (f) Pratt, W. B.; Ruddon, R. W.; Ensminger, W. D.; Maybaum, J. The Anti-Cancer Drugs, 2nd Ed., Oxford University Press: New York, 1994, pp 133–139. (g) Zou, Y.; Houten, B. V.; Farrell, N. Biochemistry 1993, 32, 9632. (h) Lippert, B. Prog Inorg Chem 1989, 37, 1. (i) Sundqvist, W. I.; Lippard, S. J. Coord Chem Rev 1990, 100, 293. (j) Reedijk, J. J Chem Soc Chem Commun 1996, 801. (k) Arpalahti, J. In: Sigel, H.; Sigel, A., eds. Metal Ions in Biological Systems, Vol. 32; Marcel Dekker, New York, 1996, pp 379–395. (l) Farrell, N. In: Sigel, H.; Sigel, A., eds. Metal Ions in Biological Systems, Vol. 32; Marcel Dekker: New York, 1996, pp 603–639. (m) van der Veer, J. L.; Reedijk, J. Chem. Br 1988, 24, 775. (n) Pinto, A. L.; Lippard, S. J. Biochem Biophys Acta 1985, 780, 167. (o) Reedijk, J. Pure Appl Chem 1987, 59, 181. (p) Lippard, S. J. Pure Appl Chem 1987, 59, 731. (q) Lippert, B. Gazz Chim Ital 1988, 118, 153. (r) Rosenberg, B. Cancer 1985, 55, 2303. (s) O'Dwyer, P. J.; Johnson, S. W.; Hamilton, T. C. In Devita, V. T.; Hellman, S.; Rosenberg, S. A., eds. Cancer: Principles and Practice of Oncology, 5th ed. Lippincott-Raven: Philadelphia, 1997, pp 418–462.
2. (a) Reedijk, J.; Lohman, P. H. M. Pharm Week Sci Ed 1985, 7, 173. (b) Prestayko, A. W.; Crooke, S. T.; Carter, S. K., eds. In: Cisplatin: Current Status and New Developments; Academic: New York, 1980. (c) Loehrer, P. J.; Einhorn, L. H. Ann Intern Med 1984, 100, 704. (d) Lim, M. C.; Martin, R. B. J Inorg Nucl Chem 1976, 38, 1911. (e) Aprile, F.; Martin, D. S., Jr. Inorg Chem 1962, 1, 551.

3. (a) Bancroft, D. P.; Lepre, C. A.; Lippard, S. J. J Am Chem Soc 1990, 112, 6860. (b) Lepre, C. A.; Lippard, S. J. Nucleic Acids and Molecular Biology, Vol. 4; Springer: Berlin, 1990, p 9. (c) Reedijk, J. Inorg Chim Acta 1992, 198, 873.

4. (a) Fichtinger-Schepman, A. M. J.; Lohman, P. H. M.; Reedijk, J. Nucl Acids Res 1982, 10, 5345. (b) Eastman, A. Biochemistry 1985, 24, 5027. (c) Fichtinger-Schepman, A. M. J.; van der Veer, J. L.; den Hartog, J. H. J.; Lohman, P. H. M.; Reedijk, J. Biochemistry 1985, 24, 707. (d) Eastman, A. Chem Biol Interact 1987, 61, 241. (e) Eastman, A. Pharmacol Ther 1987, 34, 155. (f) Johnson, N. P.; Hoeschele, J. D.; Rahn, R. O. Chem-Biol Interact 1980, 30, 151. (g) Eastman, A. Biochemistry 1983, 22, 3927. (h) Comess, K. M.; Burstyn, J. N.; Essigmann, J. M.; Lippard, S. J. Biochemistry 1992, 31, 3975. (i) Lippert, B.; Schollhorn, H.; Thewalt, U. Inorg Chim Acta 1992, 198, 723. (j) Pinto, A. L.; Naser, N. J.; Essigmann, J. M.; Lippard, S. J. J Am Chem Soc 1986, 108, 7405. (k) Eastman, A. Biochemistry, 1986, 25, 3912.

5. (a) Jones, J. C.; Zhen, W.; Reed, E.; Parker, R. J.; Sancar, A.; Bohr, V. A. J Biol Chem 1991, 266, 7101. (b) Zhen, W.; Link, C. J., Jr.; O'Connor, P. M.; Reed, E.; Parker, R. J.; Howell, S. B.; Bohr, V. A. Mol Cell Biol 1992, 12, 3689. (c) Corda, Y.; Job, C.; Anin, M. F.; Leng, M.; Job, D. Biochemistry 1993, 32, 8582.

6. (a) Milburn, G. H. W.; Truter, M. R. J Chem Soc A 1966, 1609. (b) Raudaschl, G.; Lippert, B.; Hoeschele, J. D.; Howard-Lock, H. E.; Lock, C. J. L.; Pilon, P. Inorg Chim Acta 1985, 106, 141. (c) Faggiani, R.; Lippert, B.; Lock, C. J. L.; Rosenberg, B. Inorg Chem 1977, 16, 1192. (d) Faggiani, R.; Lippert, B.; Lock, C. J. L.; Rosenberg, B. J Am Chem Soc 1977, 99, 777. (e) Gust, R.; Schonenberger, H.; Kritzenberger, J.; Range, K.-J.; Klement, U.; Burgemeister, T. Inorg Chem 1993, 32, 5939. (f) Sherman, S. E.; Gibson, D.; Wang, A. H.-J.; Lippard, S. J. J Am Chem Soc 1988, 110, 7368. (g) Bloemink, M. J.; Engelking, H.; Karentzopoulos, S.; Krebs, B.; Reedijk, J. Inorg Chem 1996, 35, 619. (h) Talman, E. G.; Bruning, W.; Reedijk, J.; Spek, A. L.; Veldman, N. Inorg Chem 1997, 36, 854. (i) Connick, W. B.; Marsh, R. E.; Schaefer, W. P.; Gray, H. B. Inorg Chem 1997, 36, 913. (j) Vicente, J.; Chicote, M. T.; Beswick, M. A.; de Arellano, M. C. R. Inorg Chem 1996, 35, 6592. (k) Hitchcock, A. P.; Lock, C. J. L.; Lippert, B. Inorg Chim Acta 1986, 124, 101. (l) Sugiura, C. J Phys Soc Jpn 1990, 59, 2134. (m) Sugiura, C.; Muramatsu, S. J Phys Chem Solids 1985, 46, 1215. (n) Mazalov, L. N.; Voityuk, A. A.; Kravtsova, E. A. J Struct Chem 1981, 22, 169. (o) Wei, C. H.; Hingerty, B. E.; Busing, W. R. Acta Crystallogr 1989, 45C, 26. (p) Alston, D. R.; Stoddart, J. F.; Williams, D. J. J Chem Soc Chem Commun 1985, 532. (q) Miller, S. E.; Wen, H.; House, D. A.; Robinson, W. T. Inorg Chim Acta 1991, 184, 111. (r) Colamarino, P.; Orioli, P. L. J Chem Soc Dalton Trans 1975, 1656. (s) Cini, R.; Caputo, P. A.; Intini, F. P.; Natile, G. Inorg Chem 1995, 34, 1130. (t) Howard-Lock, H. E.; Lock, C. J. L.; Turner, G.; Zvagulis, M. Can J Chem 1981, 59, 2737. (u) Graves, B. J.; Hodgson, D. J.; Kralingen, C. G. v.; Reedijk, J. Inorg Chem 1978, 17, 3007. (v) Kubiak, M.; Jaworska, J. K. Acta Crystallogr 1986, 42C, 1703. (w) Iball, J.; Scrimgeour, S.N. Acta Crystallogr 1977, 33B, 1194. (x) Lock, C. J. L.; Speranzini, R. A.; Zvagulis, M. Acta Crystallogr 1980, 36B, 1789. (y) Dion, C.; Beauchamp, A. L.; Rochon, F. D.; Melanson, R. Acta Crystallogr 1989, 45C, 852. (z) Rochon, F. D.; Melanson, R. Acta Crystallogr 1986, 42C, 1291. (aa) Lock, C. J. L.; Zvagulis, M. Inorg Chem 1981, 20, 1817. (ab) Barnes, J. C.; Iball, J.; Weakley, T. J. R. Acta Crystallogr 1975, 31B, 1435.

7. (a) Huang, H.; Zhu, L.; Reid, B. R.; Drobny, G. P.; Hopkins, P. B. Science 1995, 270, 1842. (b) Schroder, G.; Kozelka, J.; Sabat, M.; Fouchet, M. H.; Pfnur, R. B.; Lippert, B. Inorg Chem 1996, 35, 1647. (c) Takahara, P. M.; Rosenzweig, A. C.; Frederick, C. A.; Lippard, S. J. Nature 1995, 377, 649.

8. Pyykko, P. Chem Rev 1988, 88, 563.

9. (a) Stevens, W. J.; Krauss, M.; Basch, H.; Jasien, P. G. Can J Chem 1992, 70, 612. (b) Stevens, W. J.; Basch, H.; Krauss, M. J Chem Phys 1984, 81, 6026. (c) Krauss, M.; Stevens, W. J. Annu Rev Phys Chem 1984, 35, 357. (d) Wadt, W. R.; Hay, P. J. J Chem Phys 1985, 82, 284. (e) Hay, P. J.; Wadt, W. R. J Chem Phys 1985, 82, 299. (f) Hay, P. J.; Wadt, W. R. J Chem Phys 1985, 82, 270. (g) Andrae, D.; Haussermann, U.; Dolg, M.; Stoll, H.; Preuss, H. Theor Chim Acta 1990, 77, 123. (h) Ross, R. B.; Powers, J. M.; Atashroo, T.; Ermler, W. C.; LaJohn, L. A.; Christiansen, P. A. J Chem Phys 1990, 93, 6654.

10. Carloni, P.; Andreoni, W.; Hutter, J.; Curioni, A.; Giannozzi, P.; Parrinello, M. Chem Phys Lett 1995, 234, 50. (b) Basch, H.; Krauss, M.; Stevens, W. J.; Cohen, D. Inorg Chem 1985, 24, 3313. (c) Basch, H.; Krauss, M.; Stevens, W. J.; Cohen, D. Inorg Chem 1986, 25, 684. (d) Miller, K. J.; Taylor, E. R.; Basch, H.; Krauss, M.; Stevens, W. J. J Biomol Struct Dynam 1985, 2, 1157. (e) Barnett, G. Molec Pharmacol 1986, 29, 378. (f) Hambley, T. W. Inorg Chem 1988, 27, 1073. (g) Hambley, T. W. Inorg Chem 1991, 30, 937. (h) Kozelka, J.; Chottard, J.-C. Biophys Chem 1990, 35, 165. (i) Hambley, T. W.; Ling, E. C. H.; Messerle, B. Inorg Chem 1996, 35, 4663. (j) Kozelka, J.; Savinelli, R.; Berthier, G.; Flament, J.-P.; Lavery, R. J Comput Chem 1993, 11, 45. (k) Kozelka, J.; Petsko, G. A.; Lippard, S. J.; Quigley, G. J. J Am Chem Soc 1985, 107, 4079. (l) Yao, S.; Plastaras, J. P.; Marzilli, L. G. Inorg Chem 1994, 33, 6061. (m) McCarthy, S. L.; Hinde, R. J.; Miller, K. J.; Anderson,J. S.; Basch, H.; Krauss, M. Biopolymers 1990, 29, 823. (n) Jespersen, M.-B. K.; Altonen, A. Inorg Chem 1987, 26, 2084. (o) Navarro, J. A. R.; Romero, M. A.; Salas, J. M.; Quiros, M.; Bahraoui, J. E.; Molina, J. Inorg Chem 1996, 35, 7829. (p) Tulub, A. A. Russ J Inorg Chem 1992, 36, 1332. (q) Nikolov, G. St.; Trendafilova, N.; Schoenenberger, H.; Gust, R.; Kritzenberger, J.; Yersin, H. Inorg Chim Acta 1994, 217, 159. (r) Zuloaga, F.; Perez, R. A. J Phys Chem 1986, 90, 4491. (s) Palkin, V. A.; Kuzina, T. A. Russ J Inorg Chem 1992, 37, 2314. (t) Allured, V. S.; Kelly, C. M.; Landis, C. R. J Am Chem Soc 1991, 113, 1. (u) Louwen, J. N.; Hengelmolen, R.; Grove, D. M.; Stufkens, D. J.; Oskam, A. J Chem Soc Dalton Trans 1986, 141. (v) Yakovlev, V. N.; Panina, N. S.; L'vovskii, V. E. J Struct Chem 1991, 32, 22. (w) Hambley, T. W. Inorg Chim Acta 1987, 137, 15. (x) Kozelka, J.; Petsko, G. A.; Quigley, G. J.; Lippard, S. J. Inorg Chem 1986, 25, 1075. (y) Cundari, T. R.; Fu, W.; Moody, E. W.; Slavin, L. L.; Snyder, L. A.; Sommerer, S. O.; Klinckman, T. R. J Phys Chem 1996, 100, 18057. (z) Tornaghi, E.; Andreoni, W.; Carloni, P.; Hutter, J.; Parrinello, M. Chem Phys Lett 1995, 246, 469. (aa) Lipinski, J. Inorg Chim Acta 1988, 152, 151.

11. The proprietary software of BioNumerik Pharmaceuticals, Inc., has modules to run both quantum-mechanical and statistical mechanics procedures.

12. Frisch, M. J.; Trucks, G. W.; Schlegel, H. B.; Gill, P. M. W.; Johnson, B. G.; Robb, M. A.; Cheeseman, J. R.; Keith, T.; Peterson, G. A.; Montgomery, J. A.; Raghavachari, K.; A.-Laham, M. A.; Zakrzawski, V. G.; Ortiz, J. V.; Foresman, J. B.; Cioslowski, J.; Stefanov, B. B.; Nanayakkara, A.; Challa-

combe, M.; Peng, C. Y.; Ayala, P. Y.; Chen, W.; Wong, M. W.; Andres, J. L.; Replogle, E. S.; Gomperts, R.; Martin, R. L.; Fox, D. J.; Binkley, J. S.; DeFrees, D. J.; Baker, J.; Stewart, J. P.; H.-Gordon, M.; Gonzalez, C.; Pople, J. A. GAUSSIAN-94, Rev. C.2, Gaussian, Inc., Pittsburgh, PA, 1995.

13. Schmidt, M. W.; Baldridge, K. K.; Boatz, J. A.; Elbert, S. T.; Gordon, M. S.; Jensen, J. H.; Koseki, S.; Matsunaga, N.; Nguyen, K. A.; Su, S. J.; Windus, T. L.; Dupuis, M.; Montgomery, J. A.; J Comput Chem 1993, 14, 1347.
14. (a) Binkley, J. S.; Pople, J. A.; Hehre, W. J. J Am Chem Soc 1980, 102, 939. (b) Gordon, M. S.; Binkley, J. S.; Pople, J. A.; Pietro, W. J.; Hehre, W. J. J Am Chem Soc 1982, 104, 2797. (c) Pietro, W. J.; Francl, M. M.; Hehre, W. J.; DeFrees, D. J.; Pople, J. A.; Binkley, J. S. J Am Chem Soc 1982, 104, 5039.
15. (a) Ditchfield, R.; Hehre, W. J.; Pople, J. A. J Chem Phys 1971, 54, 724. (b) Hehre, W. J.; Ditchfield, R.; Pople, J. A. J Chem Phys 1972, 56, 2257. (c) Francl, M. M.; Pietro, W. J.; Hehre, W. J.; Binkley, J. S.; Gordon, M. S.; Defrees, D. J.; Pople, J. A. J Chem Phys 1982, 77, 3654. (d) Hariharan, P. C.; Pople, J. A. Theor Chim Acta 1973, 28, 213. (e) Hariharan, P. C.; Pople, J.A. Mol Phys 1974, 27, 209. (f) Gordon, M. S. Chem Phys Lett 1980, 76, 163. (g) Dill, J. D.; Pople, J. A. J Chem Phys 1975, 62, 2921. (h) Binkley, J. S.; Pople, J. A. J Chem Phys 1977, 66, 879.
16. (a) Mclean, A. D.; Chandler, G. S. J Chem Phys 1980, 72, 5639. (b) Krishnan, R.; Binkley, J. S.; Seeger, R.; Pople, J. A. J Chem Phys 1980, 72, 650.
17. (a) Clark, T.; Chandrasekhar, J.; Spitznagel, G. W.; Schleyer, P. v. R. J Comput Chem 1983, 4, 294. (b) Frisch, M. J.; Pople, J. A.; Binkley, J. S. J Chem Phys 1984, 80, 3265.
18. Dunning, T. H. Jr.; Hay, P. J. In: Schaefer, H. F., ed. Modern Theoretical Chemistry; Plenum, New York, 1976, pp. 1–28.
19. (a) Woon, D. E.; Dunning, T. H. Jr. J Chem Phys 1993, 98, 1358. (b) Kendall, R. A.; Dunning, T. H. Jr.; Harrison, R. J. J Chem Phys 1992, 96, 6796. (c) Dunning, T. H. Jr.; J Chem Phys 1989, 90, 1007.
20. Møller, C.; Plesset, M. S. Phys Rev 1934, 46, 618.
21. (a) Hoffmann, R.; Lipscomb, W. N. J Chem Phys 1962, 36, 2179. (b) Hoffmann, R. J Chem Phys 1963, 39, 1397.
22. Mealli, C.; Proserpio, D. M. J Chem Educ 1990, 67, 399.
23. Fujimoto, H.; Hoffmann, R. J Phys Chem 1974, 78, 1167.
24. (a) Bader, R. F. W. Atoms in Molecules. A Quantum Theory, Clarendon: Oxford, 1990. (b) B.-Konig, F. W.; Bader, R. F. W.; Tang, T.-H. J Comput Chem 1982, 3, 317 (modified by T. A. Keith and J. R. Cheeseman). (c) Bader, R. F. W. Chem Rev 1991, 91, 893.
25. (a) Chatt, J.; Duncanson, L.; Venanzi, L. J Chem Soc 1955, 4461. (b) Duncanson, L.; Venanzi, L. J Chem Soc 1960, 3841. (c) Chatt, J.; Duncanson, L.; Shaw, B.; Venanzi, L. Disc Faraday Trans 1958, 26, 131. (d) Chatt, J.; Duncanson, L.; Guy, R. Nature 1959, 184, 526.
26. (a) Greenwood, N. N.; Earnshaw, A. E. Chemistry of Elements; Pergamon: London, 1984, p 65. (b) Rivas, J. C. M.; Brammer, L. Inorg Chem 1998, 37, 4756.
27. Casas, J. M.; Falvello, L. R.; Fornies, J.; Martin, A.; Welch, A. J. Inorg Chem 1996, 35, 6009.
28. (a) Nakamoto, K.; McCarthy, P. J.; Fujita, J.; Condrate, R. A.; Behnke, G. T. Inorg Chem 1965, 4, 36. (b) Clark, R. J. H.; Williams, C. S. J Chem Soc A 1966, 1425. (c) Barrow, G. M.; Krueger, R. H.; Basolo, F. J Inorg Nucl Chem 1956, 2, 340. (d) Mizushima, S.-I.; Nakagawa, I.; Schmelz, M. J.; Curran, C.; Quagliano, J. V. Spectrochim Acta 1958, 13, 31. (e) Adams, D. M.; Chatt, J.; Gerratt, J.; Westland, A. D. J Chem Soc A 1964, 734. (f) Powell, D. B. J Chem Soc 1956, 4495. (g) Appleton, T. G.; Clark, H. C.; Manzer, L. E. Coord Chem Rev 1973, 10, 335. (h) Powell, D. B.; Sheppard, N. J Chem Soc 1956, 3108. (i) Burgina, E. B.; Yurchenko, E. N.; Konovalov, L. V. J Struct Chem 1988, 29, 38. (j) Konovalov, L. V.; Kukushkin, V. Y.; Bel'skii, V. K.; Konovalov, V. E. Russ J Inorg Chem 1990, 35, 1523. (k) Roe, S. P.; Hill, J. O.; Magee, R. J. Inorg Chim Acta 1986, 115, L15. (l) Degen, I. A.; Rowlands, A. J. Spectrochim Acta 1991, 47A, 1263. (m) Kritzenberger, J.; Zimmermann, F.; Wokaun, A. Inorg Chim Acta 1993, 210, 47.
29. For more information on this subject, refer to ref. 24.
30. Koch, U.; Popelier, P. L. A. J Phys Chem 1995, 99, 9747.